White Rose Research Online

eprints@whiterose.ac.uk
https://eprints.whiterose.ac.uk
Universities of Leeds, Sheffield and York

Deposited via The University of Leeds.

White Rose Research Online URL for this paper:
https://eprints.whiterose.ac.uk/id/eprint/80702/

Version: Accepted Version

---

**Article:**
Nova, A, Taylor, DJ, Blacker, AJ et al. (2014) Computational studies explain the importance of two different substituents on the chelating bis(amido) ligand for transfer hydrogenation by bifunctional Cp*Rh(III) catalysts. Organometallics, 33 (13). 3433 - 3442. ISSN: 0276-7333

https://doi.org/10.1021/om500356e

---

**Reuse**
Items deposited in White Rose Research Online are protected by copyright, with all rights reserved unless indicated otherwise. They may be downloaded and/or printed for private study, or other acts as permitted by national copyright laws. The publisher or other rights holders may allow further reproduction and re-use of the full text version. This is indicated by the licence information on the White Rose Research Online record for the item.

**Takedown**
If you consider content in White Rose Research Online to be in breach of UK law, please notify us by emailing eprints@whiterose.ac.uk including the URL of the record and the reason for the withdrawal request.

# Computational studies explain the importance of two different substituents on the chelating bis(amido) ligand for transfer hydrogenation by bifunctional Cp*Rh(III) catalysts

Ainara Nova,[a,b] David J. Taylor,[c] A. John Blacker,[d] Simon B. Duckett,[c] Robin N. Perutz,[c,*] and Odile Eisenstein[a,b,*]

[a] Institut Charles Gerhardt, UMR 5253 CNRS-UM2, cc 1501, Université Montpellier 2, Place Eugène Bataillon, 34095 Montpellier, France. E-mail: Odile.Eisenstein@univ-montp2.fr

[b] Centre for Theoretical and Computational Chemistry (CTCC) Department of Chemistry, University of Oslo, P.O. Box 1033 Blindern, 0315 Oslo, Norway.

[c] Department of Chemistry, The University of York, Heslington, York, UK YO10 5DD.

[d] School of Chemistry, University of Leeds, Leeds, UK LS2 9JT

e-mail: odile.eisenstein@univ-montp2.fr and robin.perutz@york.ac.uk

**ABSTRACT:** A computational approach (DFT-B3PW91) is used to address previous experimental studies (*Chem Commun.* **2009**, 6801) that showed that transfer hydrogenation of a cyclic imine by $Et_3N{\cdot}HCO_2H$ catalyzed by 16-electron bifunctional $Cp^*Rh^{III}(XNC_6H_4NX')$, is faster when $XNC_6H_4NX' = TsNC_6H_4NH$ than when $XNC_6H_4NX' = HNC_6H_4NH$ or $TsNC_6H_4NTs$ ($Cp^* = \eta^5\text{-}C_5Me_5$, Ts = toluenesulfonyl). The computational study also considers the role of the formate

complex observed experimentally at low temperature. Using a model of the experimental complex in which Cp* is replaced by Cp and Ts by benzenesulfonyl (Bs), the calculations reveal that dehydrogenation of formic acid generates $CpRh^{III}H(XNC_6H_4NX'H)$ via an outer-sphere mechanism. The 16-electron Rh complex + formic acid are shown to be at equilibrium with the formate complex, but the latter lies outside the pathway for dehydrogenation. The calculations reproduce the experimental observation that the transfer hydrogenation reaction is fastest for the non-symmetrically substituted complex $CpRh^{III}(XNC_6H_4NX')$ (X = Bs and X′ = H). The effect of the linker between the two N atoms on the pathway is also considered. The Gibbs energy barrier for dehydrogenation of formic acid is calculated to be much lower for $CpRh^{III}(XNCHPhCHPhNX')$ than for $CpRh^{III}(XNC_6H_4NX')$ for all combinations of X and X′. The energy barrier for hydrogenation of the imine by the rhodium hydride complex is much higher than the barrier for hydride transfer to the corresponding iminium ion, in agreement with mechanisms proposed for related systems on the basis of experimental data. Interpretation of the results by MO and NBO analyses show that the most reactive catalyst for dehydrogenation of formic acid contains a localized Rh–NH π bond that is associated with the shortest Rh–N distance in the corresponding 16-electron complex. The asymmetric complex $CpRh^{III}(BsNC_6H_4NH)$ is shown to generate a good bifunctional catalyst for transfer hydrogenation because it combines an electrophilic metal center and a nucleophilic NH group.

## INTRODUCTION

The term transfer hydrogenation refers to a process that transfers two hydrogen atoms from one molecule to another via a catalyst and is distinct from typical hydrogenations employing $H_2$. This process has been successfully applied in the catalytic oxidation/reduction of ketones, imines and related organic substrates and has permitted major advances in stereoselective hydrogenation.[1-4] Most of the developments have been carried out with platinum group metals such as Ru, Rh and Ir but recent studies have shown that similar reactions and selectivity can be achieved with Fe complexes.[5] In these processes, the substrate may bind to the metal center (an inner sphere mechanism)[6] or may interact with the ligands without binding to the metal (an outer sphere mechanism).[2, 3] Considerable effort has been devoted to understand these mechanisms and experimental and computational studies have concurred to show the prevalence of the outer sphere mechanism.[2, 7-21] In the latter case, the proton is transferred from the hydrogen donor to a ligand that has an electron rich atom such as nitrogen or oxygen and the hydride is transferred to the metal. The catalyst is considered as bifunctional since it involves the metal and the ligand in the transformation between its unsaturated 16 electron (16e) and saturated 18e metal hydride forms. In the subsequent step the proton and hydride are transferred from the 18e complex to the hydrogen acceptor, while the catalyst returns to its original 16e form. The proton acceptor and the hydride acceptor can be linked by a direct bond (M–L) as found in the Noyori catalyst,[2a] or they can be separated as in the Shvo catalyst (M/L).[3] The process with the first family is exemplified in Scheme 1 for a Cp*Rh system, where transfer hydrogenation occurs from formic acid[22] or alcohol to an aldehyde, ketone or imine. In their 16e unsaturated forms, these bifunctional catalysts typically contain a bis(amido) ligand which contributes one NH ligand and

one NR ligand with a strongly electron withdrawing substituent such as NTs (Ts = 4-toluenesulfonyl).

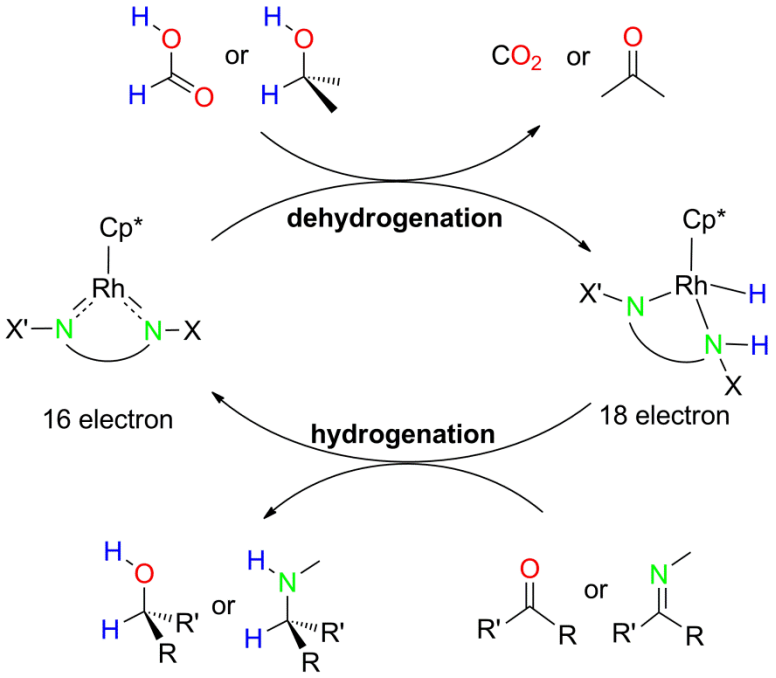


**Scheme 1.** Hydrogen transfer processes exemplified by bifunctional Cp*Rh(XN–NX′) catalysts, where X is usually H or alkyl, X' is usually arenesulfonyl, and R, R' are H or hydrocarbyl.

In many catalysts, the 16e metal complex is in the bis(amido) form and is stabilized by a π-bond to at least one amido group.[2c, 11, 23] On conversion to the 18e form, the amido group is protonated to form an amine and the empty metal site occupied by a hydride. Often, the 18e form is isolated with another anionic donor such as chloride in place of the hydride and this derivative can be used as precursor for the transfer hydrogenation reaction. For instance, this is the case for Cp*MCl(1,2-$TsNC_6H_{10}PhNH_2$) (M = Rh, Ir; $C_6H_{10}$ = 1,2-$C_6H_{10}$-),[24] (*p*-cymene)RuCl(1,2-$TsNCHPhCHPhNH_2$),[25] and Cp*RhCl(1,2-$TsNCHPhCHPhNH_2$).[26, 27] In rare cases, the catalyst has been isolated in both its active 16e and 18e forms. For example, the 18e (*p*-cymene)RuH(1,2-$TsNCHPhCHPhNH_2$), and the corresponding unsaturated

16e form were isolated and both shown to mediate transfer hydrogenation.[25] Likewise, the 18e Cp*IrH(1,2-TsNCHPhCHPhNH$_2$) has been characterized together with its 16e unsaturated form and both have been shown to be catalytically active in transfer hydrogenation, but only the 16e derivative has been isolated when $Ir^{III}$ is replaced by $Rh^{III}$.[28] Computational studies have been concerned with dehydrogenation of sacrificial alcohol or hydrogenation of ketones, with the focus in this latter case on asymmetric induction. The calculations have shown that these catalysts operate via an outer-sphere mechanism with a concerted transition state.[8-12, 19] The energy barrier for transfer hydrogenation is usually lowered by the presence of explicit solvent molecules representing water or alcohol, which stabilize the polar bonds via H bonding.[13, 14, 17-19, 21]

A combined experimental/ computational study of the reaction in aqueous solution also shows that water slightly lower the energy barriers.[29] Dynamic ab initio studies of the reaction have shown that a protic solvent can assist by storing and delivering protons, thereby making the transfer hydrogenation reaction non-concerted.[13, 17] However, the participation of the solvent in proton transfer does not modify the M···H···C geometry of the TS for hydride transfer significantly. A typical concerted transition state is shown below.

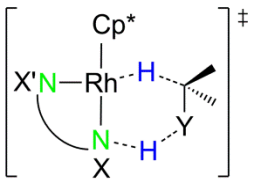


If catalytic activity is reduced, the study of the mechanism may become easier and the chances of isolating significant reaction intermediates increase. Wills *et al.* demonstrated a marked reduction in catalytic rate by replacing the $NH_2$ group of a ruthenium amido amine transfer hydrogenation catalyst by an N(alkyl)$_2$ group, thus

blocking part of the standard mechanism and forcing the amido (NTs) group to become involved in the proton transfer relay.[30] Transfer hydrogenation is also slowed when the ligand TsN–CHPhCHPh–NH is replaced by the conjugated benzene derivative, TsN–$C_6H_4$–NH. Exploiting earlier syntheses,[31] we compared three closely related 16e complexes Cp*Rh($XNC_6H_4NX'$) (X = Ts, X′ = H; X = X' = Ts; X = X′ = H), which differ only by the nature of the substituents on the two amino groups.[32] The catalysts and reaction employed for this experimental system are shown in Scheme 2, together with their labels.

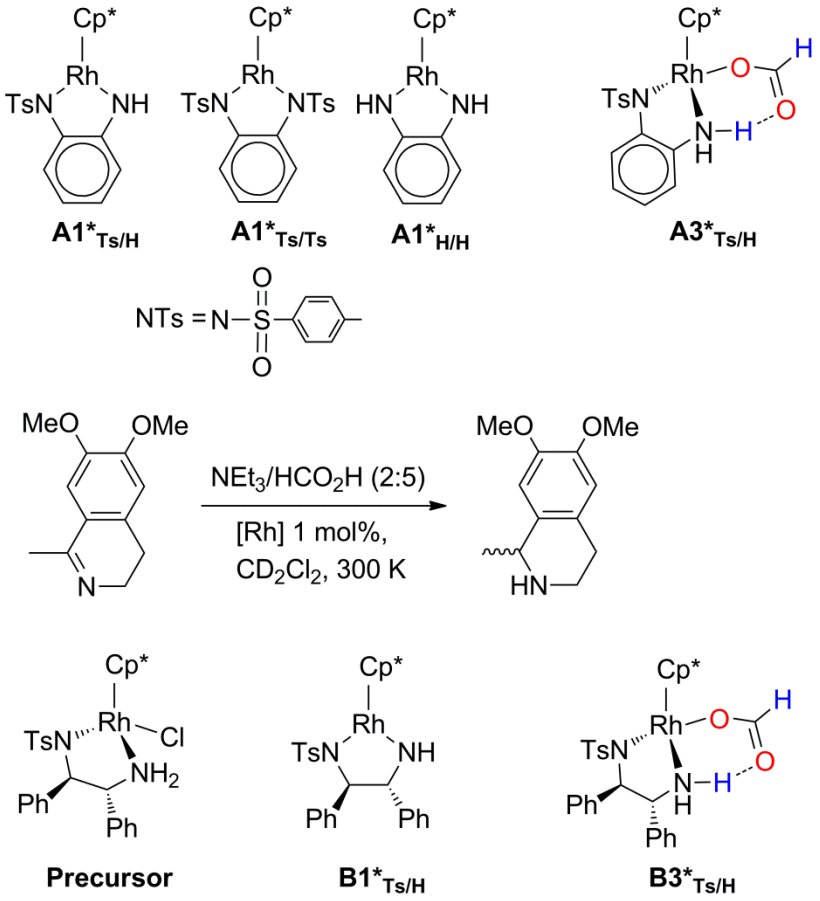


**Scheme 2.** Experimental systems (Ts = toluenesulfonyl, $SO_2C_6H_4Me$)

Structural analysis of Cp*Rh($XNC_6H_4NX'$) by X-ray diffraction and DFT calculations shows that the Rh–Cp* centroid direction is coplanar with the two Rh–N bonds.[32] This planar coordination of Rh is supported by Rh–N bond distances that are shorter (Rh–N π-interactions stronger) for NH than NTs. The catalytic activity of these complexes in the hydrogenation of an imine with formic acid was studied. Although it is typical to have one electron withdrawing ligand substituent in transfer hydrogenation catalysts, the complexes with zero or two electron withdrawing groups also proved to be active. It was found that **A1*$_{Ts/H}$** (X = Ts and X′ = H), delivers a higher rate of catalytic imine hydrogenation by formic acid:triethylamine (5:2) in dichloromethane solvent than **A1*$_{H/H}$** (X = X′ = H) and **A1*$_{Ts/Ts}$** (X = X′ = Ts), which have similar rates. The rates of reaction correlate with the strength of the reactive Rh–N π-bond in the unsaturated form as shown by the increase in the Rh–N bond lengths in the order **A1*$_{Ts/H}$** < **A1*$_{H/H}$** < **A1*$_{Ts/Ts}$**. However, the interpretation of this observation is not obvious because Rh–N π bonds might be expected to stabilize 16e complexes making them less reactive. The kinetics were studied in more detail with **A1*$_{Ts/H}$** as catalyst and methanol as solvent, revealing a first order dependence on [catalyst] and zero order dependence on [imine].[32] The reaction has also been studied with [Cp*$RhCl_2$]$_2$ and (1,2-TsNHCHPhCHPh$NH_2$) as a pre-catalyst. The resulting system was found to be eight times faster than **A1*$_{Ts/H}$** under the same conditions for reasons that are not yet explained.[27, 32] However, the effect of the nitrogen substituents (NH/NH or NTs/NTs) on the catalytic rate has not been investigated with the commonly used linker CHPhCHPh.[26, 27]

Morris *et al*. reported the reaction of formic acid with a 16e $Ru^{II}$ amido-amine complex producing a crystallographically characterized formate complex in which a proton is transferred to NH and a hydrogen bond is formed between the $NH_2$ group

and the carbonyl oxygen.[11] Koike and Ikariya reported a related reaction of formic acid with the 16e complex, [(*p*-cymene)Ru(TsNCHPhCHPhNH)].[33] The kinetics of conversion of the resulting formate complex to a hydride complex and $CO_2$ were determined. The reversibility of the formation of the formate complex was established by the observation that the hydride inserts $CO_2$ under 10 atm $CO_2$.[33] A formate complex Cp*Rh(OCHO)($TsNC_6H_4NH_2$) (**A3***$_{\mathbf{Ts/H}}$) was also characterized at low temperature by the reaction of **A1***$_{\mathbf{Ts/H}}$ with formic acid (Scheme 2, right). These results raise the question of the role played by formate complexes in the transfer hydrogenation mechanism and in particular whether they act as intermediates on the pathway for the formation of the 18e hydride complex.

In the present study, we use DFT calculations and models of the well-characterized **A1***$_{\mathbf{Ts/H}}$, **A1***$_{\mathbf{H/H}}$ and **A1***$_{\mathbf{Ts/Ts}}$ systems to analyze the electronic effects on transfer hydrogenation and study the role played by the **A3***$_{\mathbf{Ts/H}}$ formate intermediate. In addition, the effect of the N···N linker is also addressed by comparing the results obtained with models of **A1***$_{\mathbf{Ts/H}}$ to those with models of **B1***$_{\mathbf{Ts/H}}$.

## MODELS AND COMPUTATIONAL DETAILS

The model systems employed in this study are shown in Scheme 3. The catalysts were modeled by replacing Cp* by Cp and toluenesulfonyl (Ts) by benzenesulfonyl (Bs). The X/X′ substituents are given in subscripts, the labels **A** and **B** refer to the $C_6H_4$ and CHPhCHPh linkers, respectively. The substrates for the computational system are formic acid and a cyclic imine in which the MeO substituents on the aryl ring in the experimental system are replaced by H.

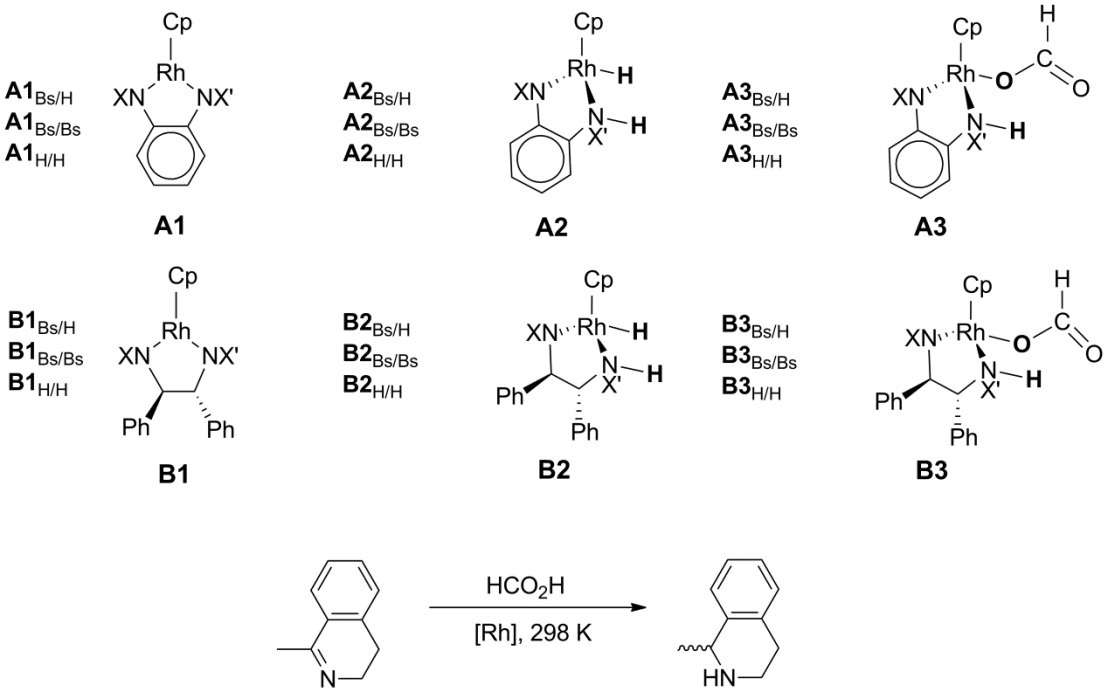


**Scheme 3.** Model systems with nomenclature (Bs = benzenesulfonyl, $SO_2Ph$)

All calculations were performed with the Gaussian03 and Gaussian09 packages[34] of programs with the hybrid B3PW91 functional.[35] The Rh atom was represented by the quasi-relativistic effective core potential SDD and the associated basis set,[36] augmented by an *f* polarization function.[37] C, H, N and O were represented by a 6-31G(*d,p*) basis set.[38] The sulfur atom was represented by an effective core potential SDD and the associated basis set,[39] augmented by a *d* polarization function.[40] Full optimization of geometries was performed without any constraints, followed by analytical calculations of the Hessian matrix to identify the nature of the located extrema as minima or transition states. Gibbs energies were obtained for $T$ = 298 K and $p$ = 1 atm within the approximation of harmonic frequencies. This methodology yields optimized structures for **A1$_{Bs/H}$**, **A1$_{H/H}$** and **A1$_{Bs/Bs}$** that are close to the corresponding X-Ray structures, as was shown in the previous study.[32] Natural bonding orbital analysis was performed with NBO version 5.0 implemented[41] in

Gaussian03. The main target of this study is to understand the relative rates observed by experiment and to relate them to the electronic effects of the different XN···NX' ligands. Since the experiments were run in an aprotic and moderately polar solvent (dichloromethane), the computations were performed for gas phase systems.

## RESULTS AND DISCUSSION

**Dehydrogenation of formic acid with $\mathbf{A1_{Bs/H}}$.** As discussed in the Introduction, the dehydrogenation of formic acid by $\mathbf{A1_{Bs/H}}$ can occur either by outer sphere transfer of two hydrogens to form the 18e hydrido complex $\mathbf{A2_{Bs/H}}$ directly, or via the intermediate formation of the formate complex $\mathbf{A3_{Bs/H}}$. This last pathway can be considered as an inner-sphere mechanism since the formate ion is directly bonded to the metal center. The Gibbs energy profiles for these two mechanisms are shown in Figure 1 in blue and red, respectively.

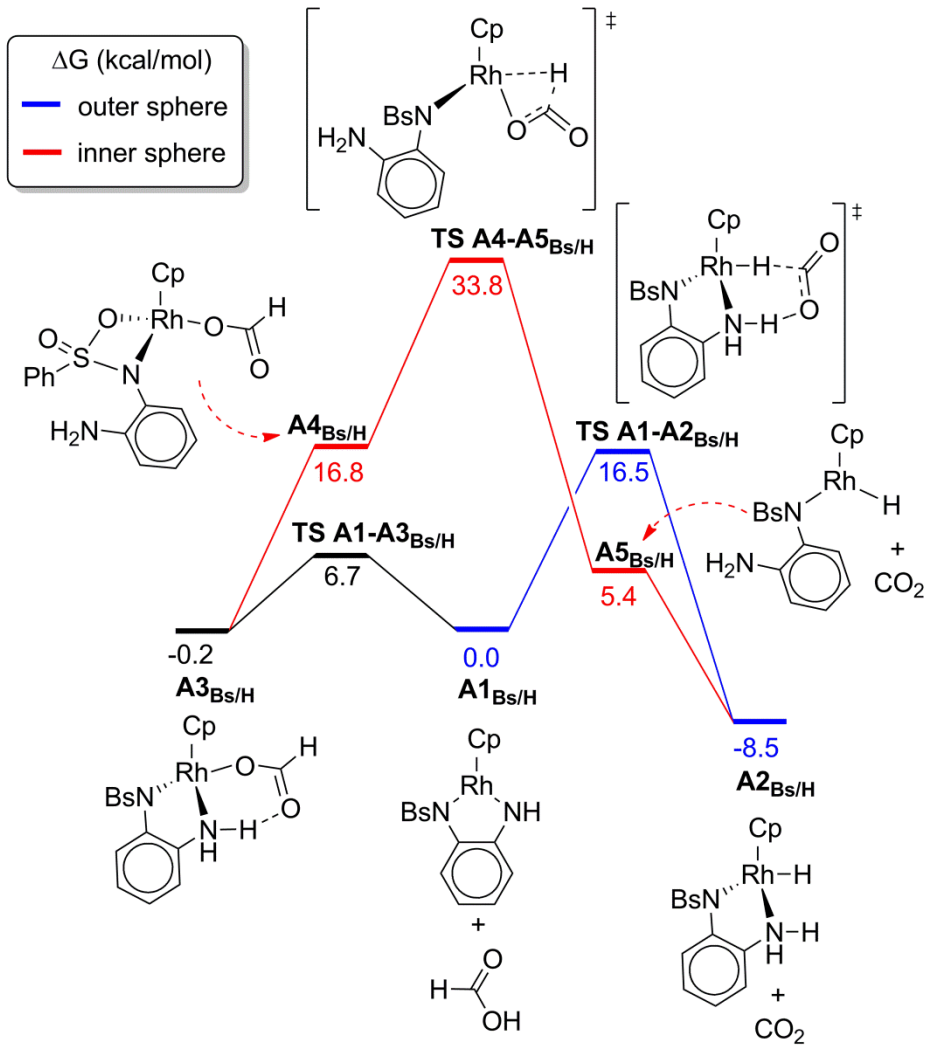


**Figure 1**. Gibbs energy profiles (kcal/mol) for the outer (blue) and inner (red) sphere dehydrogenation of formic acid with $\mathbf{A1_{Bs/H}}$ and formation of intermediate $\mathbf{A3_{Bs/H}}$ (in black).

The outer sphere hydrogen transfer from formic acid to $\mathbf{A1_{Bs/H}}$ is found to occur in a concerted manner through transition state (TS) **TS A1-A2**$_{\mathbf{Bs/H}}$ which leads directly to the final product $\mathbf{A2_{Bs/H}}$ with a Gibbs energy barrier of 16.5 kcal/mol. The transition state structure has a planar 6-membered Rh···H···C···O·· H···N ring, as already obtained in other studies.[9, 12-14, 19, 21] However in protic solvents, such as water or alcohol, it was shown that the proton transfer could be assisted by solvent and the reaction ceases to be concerted.[13]

In the present case, where the solvent ($CH_2Cl_2$) cannot act as a proton acceptor, the only assistance can be provided by triethylamine. This possibility was not studied and the Gibbs energy barrier given here is therefore likely to be an upper limiting value. The reaction of formic acid with $\mathbf{A1_{Bs/H}}$ yields complex $\mathbf{A3_{Bs/H}}$ by coordination of oxygen and transfer of a proton to nitrogen. It proceeds via a transition state, **TS A1-A3$_{Bs/H}$,** with a low Gibbs energy of 6.7 kcal/mol. The Gibbs energy of $\mathbf{A3_{Bs/H}}$ is essentially equal to that of separated $\mathbf{A1_{Bs/H}}$ and $HCO_2H$, which is consistent with the observation at low temperature of $\mathbf{A3^*_{Ts/H}}$. Scheme 4 shows that the two C–O bond distances in $\mathbf{A3_{Bs/H}}$ are consistent with a description as a rhodium $\kappa^1$-formate hydrogen-bonded to $NH_2$. Similar coordination was found in related ruthenium complexes[11, 33] and in the product of hydrogenation of $CO_2$ by an Ir pincer.[42] In the present study, the energy of $\mathbf{A3_{Bs/H}}$ is 8.3 kcal/mol above the $\mathbf{A2_{Bs/H}}$ + $CO_2$, which indicates that the dehydrogenation reaction with associated release of carbon dioxide has a favorable free energy under standard conditions.

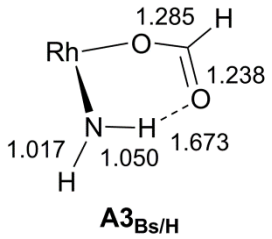


$\mathbf{A3_{Bs/H}}$

**Scheme 4**. Selected structural parameters (Å) of $\mathbf{A3_{Bs/H}}$.

The inner-sphere mechanism, shown in red in Figure 1, converts the 18e formate complex $\mathbf{A3_{Bs/H}}$ into the 18e hydride complex $\mathbf{A2_{Bs/H}}$. To evolve towards the hydride complex with associated loss of $CO_2$, $\mathbf{A3_{Bs/H}}$ starts by losing the hydrogen bond between the formate and the amine group and changing the coordination of the amido/amine ligand from $\kappa^2$-*N*,*N* to $\kappa^2$-*N*,*O* where N is the amido group and the oxygen is part of the benzenesulfonyl group at a cost of 16.8 kcal/mol. The vacancy at

the metal center required for-β-hydrogen elimination is formed concurrently with the Rh–H bond in **TS A4-A5$_{Bs/H}$**. This transition state has a Gibbs energy of 33.8 kcal/mol above reactants and yields the hydride intermediate **A5$_{Bs/H}$**. Re-coordination of the $NH_2$ group of the ligand to the Rh vacant site in **A5$_{Bs/H}$** leads to the final 18e complex **A2$_{Bs/H}$** and $CO_2$.

The energies required for the outer- and inner-sphere dehydrogenation of formic acid of 16.5 and 33.8 kcal/mol, respectively, show that an outer sphere mechanism is preferred. It follows that **A3$_{Bs/H}$** is not an intermediate within the catalytic cycle but a resting state of the transfer hydrogenation process. This also means that an outer sphere mechanism may apply even in those cases where an alkanoate/alkanoic acid (including formate) intermediate is observed.[11, 32, 33]

**Effect of the X substituents in XN–$C_6H_4$–NX' systems on dehydrogenation of formic acid by A1$_{Bs/H}$, A1$_{H/H}$, and A1$_{Bs/Bs}$.** In the hydrogenation of a cyclic imine with $NEt_3$-$HCO_2H$ using **A1*$_{Ts/H}$**, **A1*$_{H/H}$**, and **A1*$_{Ts/Ts}$** the catalytic activities were found to follow the order **A1*$_{Ts/H}$** > **A1*$_{H/H}$** ~ **A1*$_{Ts/Ts}$** (Scheme 2). Figure 2 shows the Gibbs energy profiles for reaction of the 16e species of type **A1** with formic acid via a concerted outer sphere mechanism to form the 18e hydride complexes of type **A2**. The Gibbs energy barriers for **A1$_{Bs/H}$**, **A1$_{H/H}$,** and **A1$_{Bs/Bs}$** are 16.5, 20.6, and 21.2 kcal/mol, fitting with the trend in catalytic activities (Figure 2 a-c). Formation of the hydride complexes **A2$_{Bs/H}$**, **A2$_{H/H}$**, and **A2$_{Bs/Bs}$** is exoergic by 8.5, 4.9, and 1.7 kcal/mol, respectively. In the case of the unsymmetrical **A1$_{Bs/H}$** system, protonation of the NBs group was also considered. Reaction of **A1$_{Bs/H}$** with formic acid with protonation at NBs instead of NH has a Gibbs energy barrier of 28.2 kcal/mol, which is much higher than the corresponding barrier for protonation at NH (Figure 2d). This test shows that the NBs group acts as a much less efficient proton relay than NH.

Indeed, formation of product from $\mathbf{A1_{Bs/Bs}}$ is the only endoergic process (+3.3 kcal/mol). This result is in agreement with the experiments of Wills *et al.*[30]

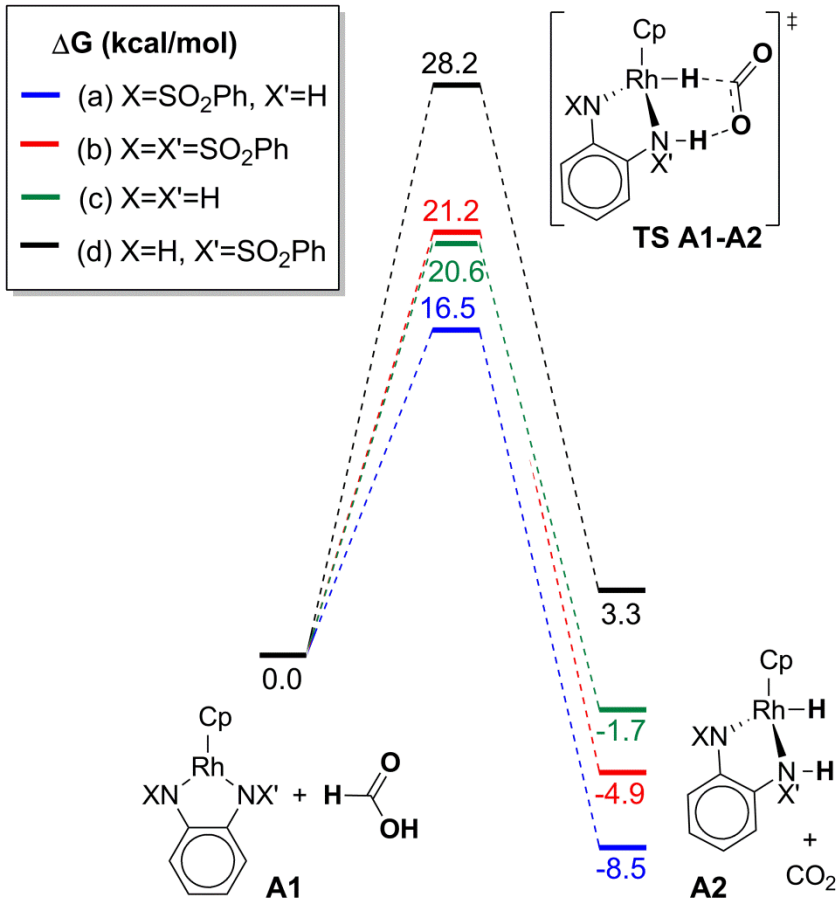


**Figure 2.** Gibbs energy profiles (kcal/mol) for the outer sphere dehydrogenation of formic acid with hydrogen transferred to: (a) the NH group for $\mathbf{A1_{Bs/H}}$, (b) an NBs ($NSO_2Ph$) group of $\mathbf{A1_{Bs/Bs}}$, (c) an NH group of $\mathbf{A1_{H/H}}$, and (d) the NBs group of $\mathbf{A1_{Bs/H}}$. See Scheme 3 for nomenclature.

**Effect of the X substituents in XN–CHPhCHPh–NX' systems on dehydrogenation of formic acid and effect of linker.** We now consider the dehydrogenation of formic acid via the outer-sphere mechanism with the flexible, saturated CHPhCHPh linker and examine the effect of the X and X' ligands on the system. We then compare the results to those obtained for the conjugated and rigid linker $C_6H_4$ in the **A1** set. Figure 3 shows that the Gibbs energy barriers increase in

the order $\mathbf{B1_{Bs/H}}$ < $\mathbf{B1_{H/H}}$ << $\mathbf{B1_{Bs/Bs}}$ with values of 3.9, 6.6, and 16.7 kcal/mol, respectively. All of these values are significantly lower than the *corresponding* values for the **A1** set of 16.5, 20.6, and 21.2 kcal/mol, respectively (Figure 2). Thus, the asymmetric substituted nitrogen ligands are associated with the lowest barriers for both the **A1** and the **B1** sets. The difference between the **A1** and **B1** sets is most marked when both the nitrogen atoms have hydrogen substituents and decreases as Bs substituents are introduced.

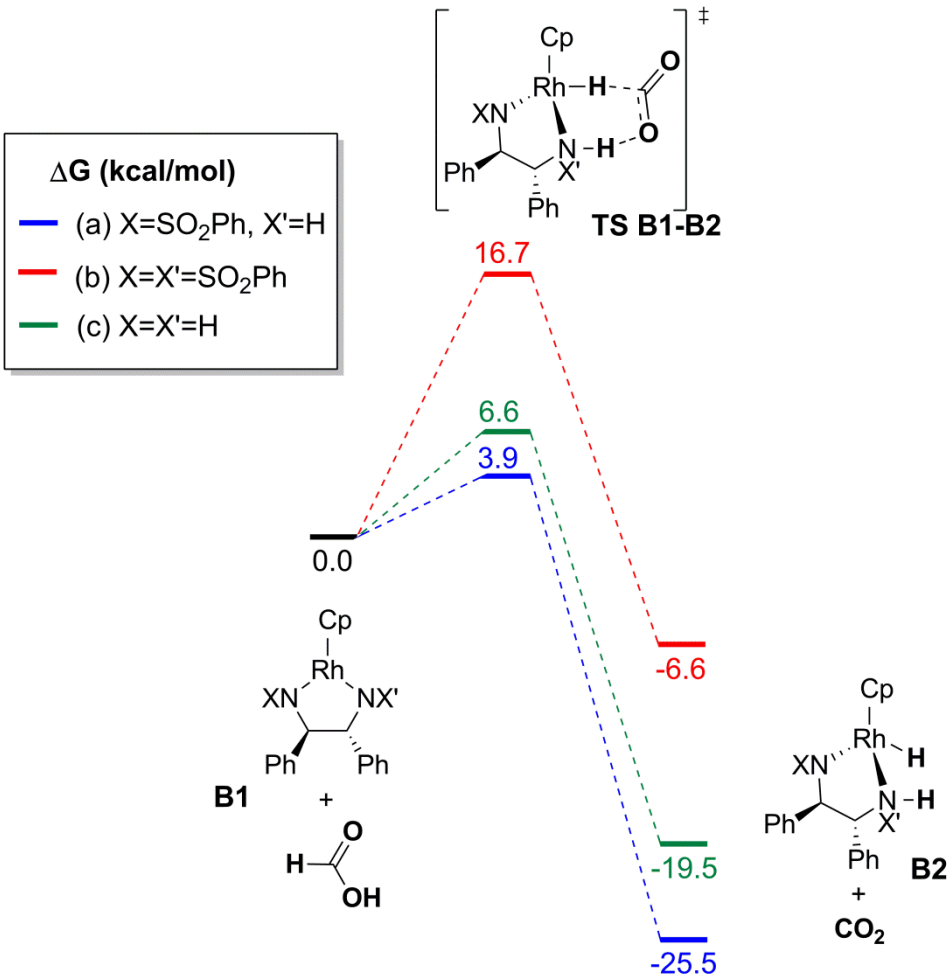


**Figure 3**. Gibbs energy profile (kcal/mol) for the outer-sphere dehydrogenation of formic acid with (a) $\mathbf{B1_{Bs/H}}$, (b) $\mathbf{B1_{Bs/Bs}}$, and (c) $\mathbf{B1_{H/H}}$.

In order to understand the origin of these differences, we compared the geometries of reactant, transition state**,** and product for the two linkers (Figure 4). The Rh–NH bond distance in $\mathbf{B1_{Bs/H}}$ with the CHPhCHPh linker is 0.037 Å shorter than with $C_6H_4$ linker, $\mathbf{A1_{Bs/H}}$. The difference is even more pronounced at the transition state (0.056 Å), but disappears in the product. Thus, the lower energy barrier is associated with the complex that has the shorter Rh–NH bond distance. The Rh–H bond is much less advanced at the transition state in **B** than in **A**, in keeping with an earlier transition state and a more exothermic reaction. Corresponding distances for the Bs/Bs and H/H series are given in Figure S1 (see Supporting Information).

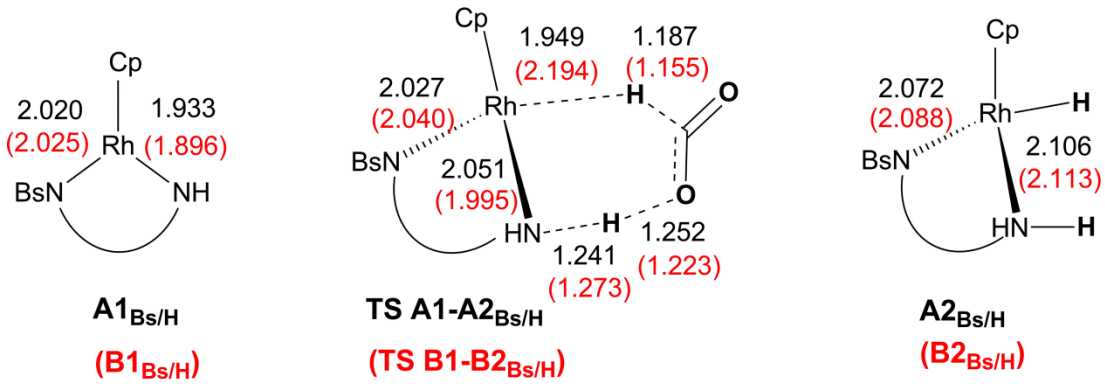


**Figure 4**. Selected bond distances (Å) shown in black for unsaturated reactant (**A1** series), transition state (**TS A1-A2**), and product (**A2** series) for the outer-sphere dehydrogenation of formic acid. Corresponding distances for saturated system **B** in red and in parentheses.

**Effect of the X substituents in XN–$C_6H_4$–NX' systems on hydrogenation of imine by $\mathbf{A2_{Bs/H}}$, $\mathbf{A2_{Bs/Bs}}$, and $\mathbf{A2_{H/H}}$.** The next stage of reaction in the transfer hydrogenation reaction is hydrogenation of the cyclic imine by the 18e hydride complexes of type **A2**. The transfer hydrogenation to the neutral imine proved to have a very high barrier. Mechanisms involving hydride attack on iminium ions have been proposed in related systems.[2b, 43, 44] We therefore considered the possibility of hydride

transfer to an iminium ion, bearing in mind that the medium is acidic. The Gibbs energy profiles for the different substituents when considering the iminium mechanism are shown in Figure 5, where the reactant and product energies correspond to the sum of the energies of the free molecules/ions. Since the starting point of Figure 5 does not match the end point of Figure 2, we reference this stage separately. The calculated Gibbs energy barriers for hydride transfer to iminium are much smaller than those for dehydrogenation of formic acid suggesting that the latter is the rate determining step. This result is also consistent with kinetic experiments on the catalytic hydrogenation of imine by $\mathbf{A^*_{Ts/H}}$ showed in Scheme 2, which proved to be zero order with respect to [imine]. The transition state is associated with a linear transit of hydride from rhodium to the iminium carbon with an almost fully formed C–H bond. The relative energies of the transition states and of the products reflect the relative hydricities of the cationic products $\mathbf{HA1^+}$.

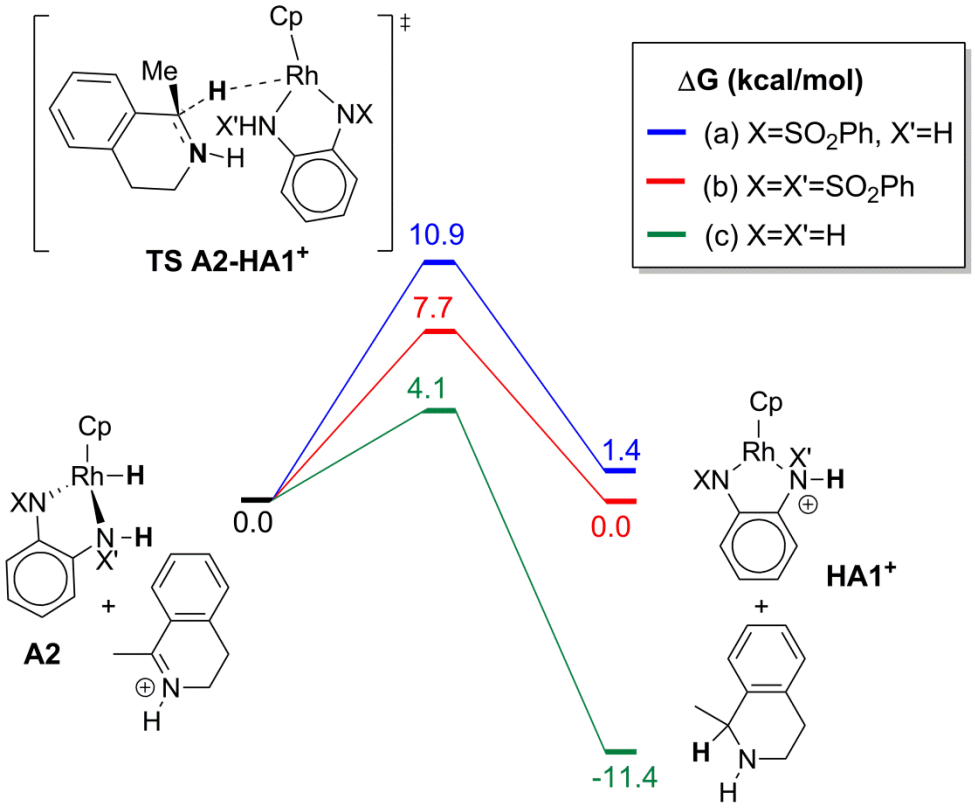

**Figure 5.** Gibbs energy profiles (kcal/mol) for the hydride transfer to iminium for systems (a) $\mathbf{A2_{Bs/H}}$, (b) $\mathbf{A2_{Bs/Bs}}$, and (c) $\mathbf{A2_{H/H}}$.

**Molecular orbital analysis of the effect of the linker, X and X' substituents.** The comparison between the $\mathbf{A1_{Bs/H}}$ and $\mathbf{B1_{Bs/H}}$ revealed the importance of the Rh–N bond length in the 16e reactant and the transition state for dehydrogenation of formic acid. The energy barrier for the dehydrogenation with $\mathbf{B1_{H/H}}$ is 14 kcal/mol lower than with $\mathbf{A1_{H/H}}$ and the Rh–N bond is 0.017 Å shorter, a pattern that is similar to that for $\mathbf{B1_{Bs/H}}$ and $\mathbf{A1_{Bs/H}}$ ($\Delta\Delta G^{\ddagger}$ = 12.6 kcal/mol, $\Delta$d = 0.037 Å). In the cases of $\mathbf{B1_{Bs/Bs}}$ and $\mathbf{A1_{Bs/Bs}}$, both $\Delta\Delta G^{\ddagger}$ (4.4 kcal/mol) and $\Delta$d (0.005 Å) are much smaller.

The interpretation of the MO interactions is facilitated by considering the more symmetrical system $\mathbf{A1_{H/H}}$ and $\mathbf{B1_{H/H}}$. Figures 6 and 7 show simplified MO diagrams of the interactions between the CpRh fragment and the ligands for HN–$C_6H_4$–NH and HN–CHPhCHPh–NH, respectively. $\mathbf{A1_{H/H}}$ and $\mathbf{B1_{H/H}}$ complexes have local $C_{2v}$ and $C_2$ symmetry, respectively. In the HN–$C_6H_4$–NH ligand (Figure 6), the out-of-plane N lone pairs combine with the π orbitals of the benzene ring leading to orbitals of $a_2$ and $b_1$ symmetry. The $a_2$ orbital is lower in energy than the $b_1$ because it involves a bonding combination of the N lone pairs and a vacant π* orbital of the benzene ring, while the $b_1$ orbital involves an antibonding combination of the N lone pairs and an occupied π orbital of benzene. The orbitals of HN–$C_6H_4$–NH enter into π interactions with the unoccupied $d_{xz}$ ($b_1$ symmetry) and the occupied $d_{xy}$ ($a_2$ symmetry) orbitals of the CpRh fragment. The occupied π orbital of $b_1$ symmetry stabilizes the 16e complex and is the HOMO, while the antibonding counterpart forms the LUMO. The combination of $a_2$ symmetry destabilizes the complex by a 4-electron repulsion.

In the HN–CHPhCHPh–NH ligand (Figure 7), there is no interaction between the CHPhCHPh orbitals and the N lone pairs with the consequence that the in-phase (*b* symmetry) and out-of phase (*a* symmetry) combinations of N lone pairs are very close in energy. In this situation, the bonding combination of the $d_{xz}$ with the *b* orbital of the ligand gives an orbital $b^+$ that is responsible for the Rh–N π bonding. It lies below the antibonding combination of the $d_{xy}$ with the *a* orbital of the ligand, which is the HOMO. The LUMO is formed by the antibonding combination of orbitals of *b* symmetry.

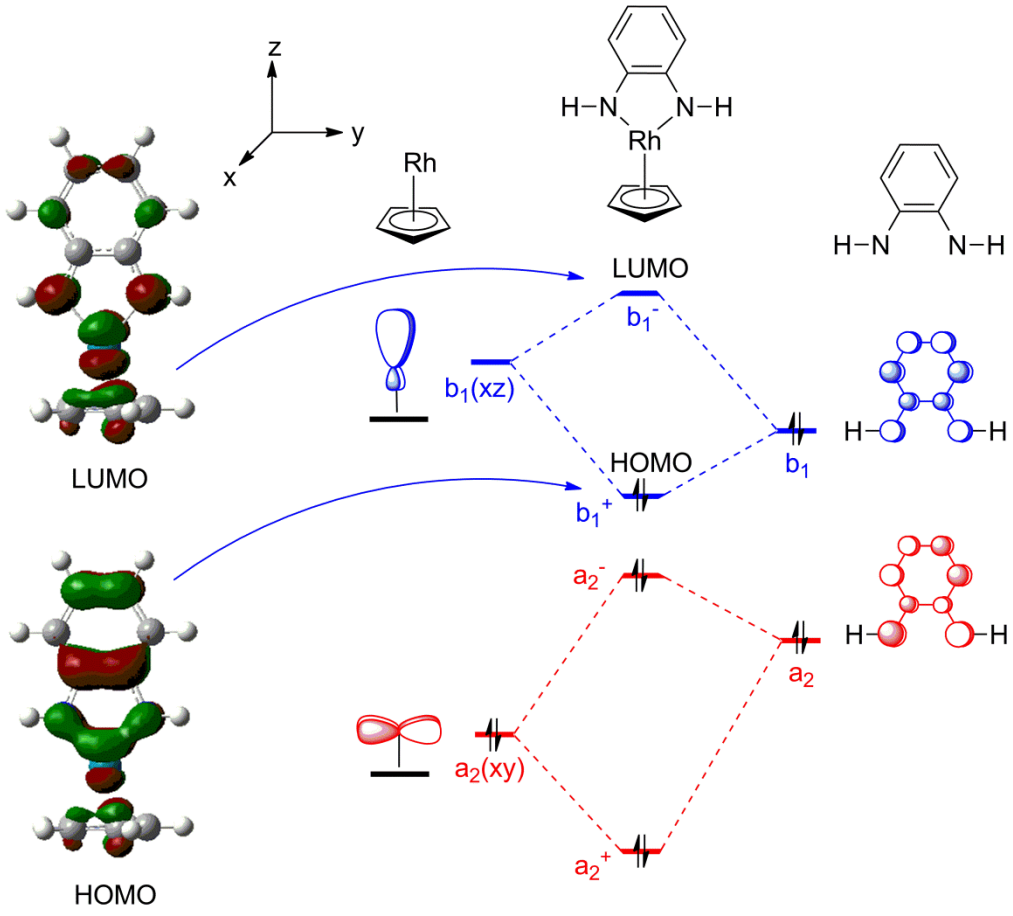


**Figure 6.** MO diagram limited to frontier orbitals for the interaction of CpRh and HN–$C_6H_4$–NH.

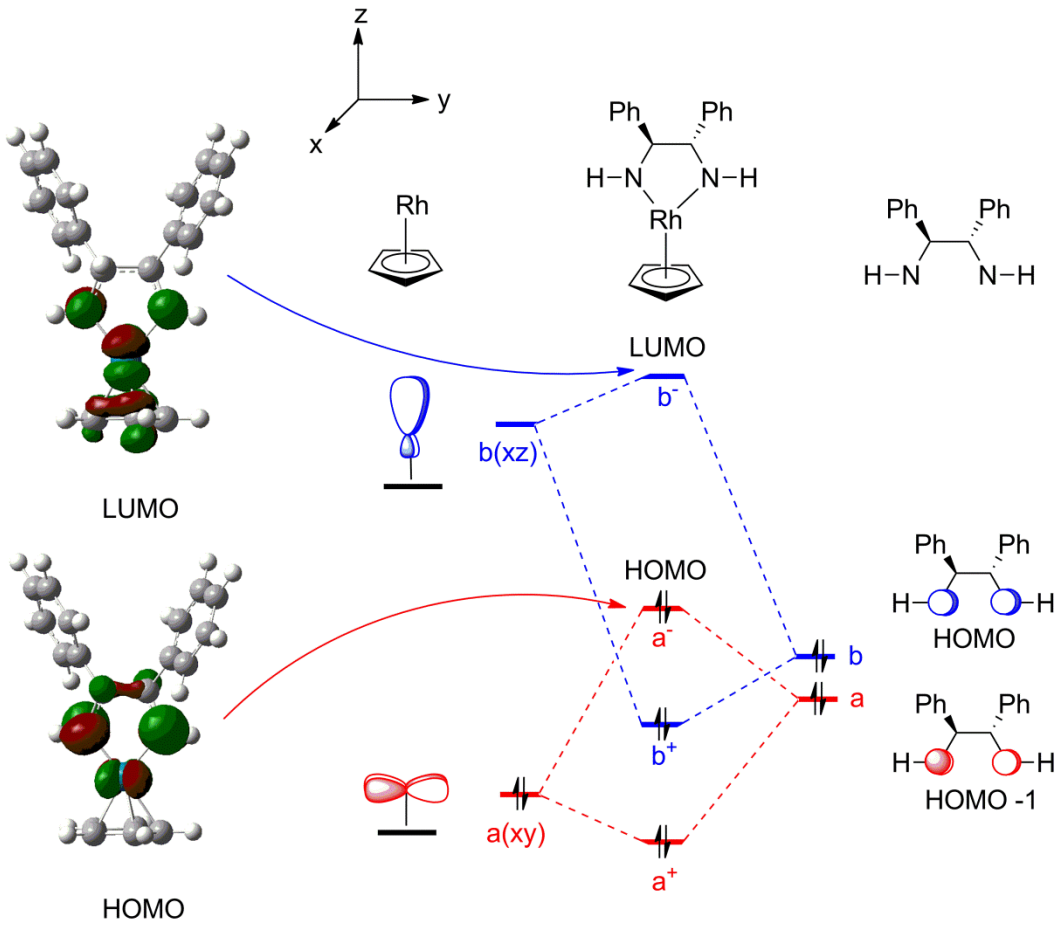


**Figure 7.** MO diagram limited to frontier orbitals for the interaction of CpRh and HN–CHPhCHPh–NH.

In CpRh(HNC$_6$H$_4$NH) and CpRh(HNCHPhCHPhNH) there is only one occupied orbital of *b* symmetry responsible for π bonding between metal and nitrogen ligand. A stronger Rh–N π bond and shorter Rh–N bond distance is expected when the N lone pairs are not delocalized as in the C$_6$H$_4$ linker, accounting for the shortening of the average Rh–N distance in **B1$_{H/H}$** (1.942 Å) relative to that in **A1$_{H/H}$** (1.959 Å). However, in the **A** system, the delocalization of the electrons of *a* symmetry through the C$_6$H$_4$ linker reduces the 4e electron repulsion between the metal and the N ligands. Consequently, it is **B1$_{H/H}$** that is more reactive towards

formic acid because the stronger 4e repulsion is relieved by the protonation at nitrogen.

In order to account for the effect of NX/NX' substituents in dehydrogenation of formic acid, an NBO analysis was performed on **A1$_{Bs/H}$**, **A1$_{Bs/Bs}$**, and **A1$_{H/H}$** and the associated transition states. The natural localized molecular orbital (NLMO) of these lone pairs (Table 1) shows their delocalization onto Rh in the different systems. For instance, in the **A1$_{Bs/H}$** system, the lone pair localized on the more basic NH has a larger metal contribution than the lone pair on NBs. The larger metal contribution is associated with a shorter Rh–N distance consistent with π-bonding. The contributions of the Rh orbital to the composition of this NLMO follow the pattern expected from the observed bond lengths: **A1$_{Bs/H}$** (NH) > **A1$_{H/H}$** > **A1$_{Bs/Bs}$** > **A1$_{Bs/H}$** (NBs).

In the transition state for dehydrogenation (**TS A1-A2**) the π-interaction is lost, as is shown by the reduction of the metal contribution to the NLMO of the reacting N in **TS A1-A2$_{Bs/H}$**, **TS A1-A2 $_{Bs/Bs}$** and **TS A1-A2 $_{H/H}$** of 1.2, 0.7, and 0.8%, respectively (Table 1, Figure 8). This means that the N recovers its nucleophilicity to interact with the proton from formic acid, which is reflected in the contribution of hydrogen in the NLMO, and the metal recovers its electrophilicity to interact with hydride from the formic acid. In this situation, the NX/NX' ligand combination that most enhances the nucleophilicity of the N and electrophilicity of the metal is NBs/NH. Paradoxically, it is the nitrogen with the shortest bond to rhodium and the most delocalized lone pair that is most nucleophilic.

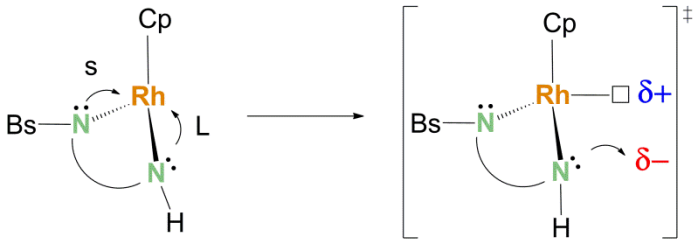


**Figure 8.** Graphical representation of the delocalization of the N lone pairs in **A1$_{Bs/H}$** and **TS A1-A2$_{Bs/H}$**. The delocalization of the NBs lone pair onto rhodium is small (s) whereas the delocalization of the NH lone pair is large (L). The square represents a vacant site.

**Table 1.** The NLMO description of the nitrogen lone pairs from the NBO analysis and Rh–N bond distances (Å) for **A1** and **TS A1-A2** series.

| Reaction Pathway | NX/NX' | **Reactant** | | | **Transition state** | | | |
|---|---|---|---|---|---|---|---|---|
| | | $\chi^N$ | $\chi^{Rh}$ | d(Rh–N) | $\chi^N$ | $\chi^{Rh}$ | $\chi^H$ | d(Rh–N) |
| **A1$_{Bs/H}$** → | NH | 69.3 | 11.5 | 1.933 | 81.2 | 1.2 | 11.9 | 2.051 |
| **TSA1-A2$_{Bs/H}$** | NBs | 78.3 | 2.8 | 2.020 | 83.5 | 2.5 | | 2.027 |
| **A1$_{Bs/Bs}$** → | NBs | 77.6 | 6.0 | 1.995 | 81.6 | 0.7 | 12.9 | 2.125 |
| **TSA1-A2$_{Bs/Bs}$** | NBs' | 77.6 | 6.0 | 1.995 | 84.3 | 1.7 | | 2.035 |
| **A1$_{H/H}$** → | NH | 68.5 | 9.2 | 1.958 | 79.1 | 0.8 | 15.7 | 2.093 |
| **TSA1-2$_{H/H}$** | NH' | 68.5 | 9.2 | 1.958 | 78.2 | 5.1 | | 1.968 |

[a] $\chi^N$, $\chi^{Rh}$, and $\chi^H$ represent the NLMO contributions to the N lone pair from N, Rh, and hydrogen from formic acid close to N.

## CONCLUSION

In this study, we have shown that in transfer hydrogenation reactions, the observation of an alkanoate species such as Cp*Rh(OCHO)(TsNC$_6$H$_4$NH$_2$) does not necessarily imply an inner sphere mechanism.[32] Indeed, this kind of complex can be present as a resting state of the catalyst at equilibrium with the active form, but not on the direct pathway for dehydrogenation. The computations show that there is a

significantly lower free energy barrier (17.3 kcal/mol) for the outer-sphere mechanism for the dehydrogenation of formic acid by CpRh(BsNC$_6$H$_4$NH) (**A1$_{Bs/H}$**) than for an inner sphere mechanism involving the formate complex **A3$_{Bs/H}$**, (the benzenesulfonyl (Bs) acts as a model for the experimental toluenesulfonyl (Ts)).

In a transfer hydrogenation process proceeding by an outer-sphere mechanism, $H^+$ and $H^-$ are transferred from one species to another. In this study we have considered the hydrogen transfer from formic acid to a Rh–NX bond in different $Rh^{III}$(XN–linker–NX') systems where X/X' are Bs/H or Bs/Bs or H/H. The calculations show that the barrier for dehydrogenation is lower for the Bs/H combination than for the others by approx 4-5 kcal/mol. For the next step, the hydrogenation of imine, occurs with a much lower barrier when hydride transfers to the iminium ion than the neutral imine. The iminium mechanism, consistent with an acidic medium, has been proposed previously.[2b, 43, 44] The resulting barriers for hydrogenation are considerably lower than for dehydrogenation of formic acid. This analysis is consistent with the kinetic study of the experimental system, which shows no dependence on the imine concentration and a modest kinetic preference for Ts/H combination.[32]

The higher reactivity of the Bs/H complex can be understood by the need to have a bifunctional system with both an electrophilic metal and a nucleophilic nitrogen to accept the $H^-$ and $H^+$ in the dehydrogenation of formic acid. This combination results in the strongest Rh–NH π bonding in the reactant in which the nitrogen lone pair of BsN does not compete with the NH lone pair.

The linker in both experimental and computational systems can be unsaturated as in C$_6$H$_4$ or saturated as in CHPhCHPh fragments. The former delocalizes the nitrogen lone pairs onto the benzene ring while the latter cannot do so. Consequently,

the system with the saturated linker exhibits-both shorter Rh–N bond distances and a built-in 4e repulsion between the Rh and the N lone pairs (Figures 6 and 7). The relief of this 4e repulsion upon dehydrogenation of formic acid results in energy barriers that are lower for the saturated linker for all X, X' combinations. The difference in the effect of 4e repulsion between the saturated and the unsaturated linker increases with the electron donation ability of the N ligand. It thus increases when the substituent on N is not electron withdrawing. The only experimental data on the saturated complexes are for the Ts/H combination, which is indeed much more active than the corresponding unsaturated system.[32] The calculations indicate that the energy barrier for the model of the latter case, $\mathbf{B1_{Bs/H}}$, is 3.9 kcal/mol compared to 16.5 kcal/mol for the unsaturated analogue $\mathbf{A1_{Bs/H}}$ (Figures 2 and 3). It might be expected that there would be further relief of repulsion with two NH units, but the calculations indicate that the barrier for $\mathbf{A1_{H/H}}$ is slightly higher (6.6 kcal/mol), probably because this species does not have sufficient electrophilic character at rhodium.

## ASSOCIATED CONTENT

**Supporting information.**

Full list of authors for reference 34. Figure with selected bond distances for **A1**, **A2** and **TS A1-A2** set and **B** analogues. Lewis structures used for the NBO analysis. List of coordinates, energies and Gibbs energies (a.u.) for all calculated systems are given in an xyz file readable by mercury. This material is available free of charge via the Internet at http://pubs.acs.org.

## AUTHOR INFORMATION

**Corresponding authors**

E-mail: robin.perutz@york.ac.uk; odile.eisenstein@univ-montp2.fr

**Notes**

The authors declare no competing financial interest

## ACKNOWLEDGMENTS

A.N. thanks the Spanish MINECO for a postdoctoral fellowship in Université Montpellier 2. A.N. and O.E. thank the support of the research Council of Norway through a Centre of Excellence Grant (Grant No. 179568/V30). O.E. thanks the CNRS and the Ministère de l'Enseignement Supérieur et de la Recherche for funding. S.B.D., R.N.P. and D.J.T. thank EPSRC and Piramal Healthcare for financial support.

## REFERENCES

(1) (a) Bhaduri, S.; Mukesh, D., *Homogeneous Catalysis: Mechanisms and Industrial Applications*; Wiley: New York, NY, 2000. (b) de Vries, J. G., Elsevier, C. J. Eds. *Handbook of Homogeneous Hydrogenations*; Wiley-VCH: Weinheim, 2007, Vol 1-3, Chapters 15, 20, 35.

(2) (a) Noyori, R. *Angew. Chem., Int. Ed.* **2002**, *41*, 2008-2022. (b) Bullock, R. M. *Chem.–Eur. J.* **2004**, *10*, 2366-2374. (c) Clapham, S. E.; Hadzovic, A.; Morris, R. H. *Coord. Chem. Rev.* **2004**, *248*, 2201-2237. (d) Samec, J. S. M.; Bäckvall, J.-E.; Andersson, P. G.; Brandt. P. *Chem. Soc. Rev.* **2006**, *35*, 237-248. (e) Ikariya, T.; Blacker, A. J. *Acc. Chem. Res.* **2007,** *40,* 1300–1308. (f) Ikariya, T.; Murata, K.; Noyori, R. *Org. Bio. Chem.* **2006**, *4*, 393-406. (g) Ito M.; Ikariya, T. *Chem. Commun.* **2007**, 5134-5142. (h) Nixon, T. D., Whittlesey, M. K.; Williams, J. M. J. *Dalton Trans.* **2009**, *5*, 753-762. (i) Ikariya, T. *Bull. Chem. Soc. Jpn.* **2011**, *84*, 1-16. (j) Eisenstein, O.; Crabtree, R. H. *New J. Chem.* **2013**, *37*, 21-27.

(3) (a) Blum, Y.; Czarkie, D.; Rahamim, Y.; Shvo, Y. *Organometallics* **1985**, *4*, 1459-1461. (b) Larsson, A. L. E.; Persson, B. A.; Bäckvall, J.-E. *Angew. Chem. Int. Ed. Eng.* **1997**, *36*, 1211-1212. (c) Laxmi, Y. R. S.; Bäckvall, J.-E. *Chem. Commun.* **2000**, 611-612. (d) Pàmies, O.; Bäckvall, J.-E. *Chem. –Eur. J.* **2001**, *7*, 5052-5058. (e) Casey, C. P.; Singer, S. W.; Powell, D. R.; Hayashi, R. K.; Kavana, M. *J. Am. Chem. Soc.* **2001**, *123*, 1090-1100. (f) Johnson, J. B.; Bäckvall, J.-E. *J. Org. Chem.* **2003**, *68*, 7681-7684. (g) Casey, C. P.; Johnson, J. B. *J. Org. Chem.* **2003**, *68*, 1998-2001. (h) Casey, C. P.; Johnson, J. B. *J. Am. Chem. Soc.*, **2005**, *127*, 1883-1894. (i) Casey, C. P.; Johnson, J. B.; Singer, S. W.; Cui, Q. *J. Am. Chem. Soc.*, **2005**, *127*, 3100-3109 Correction *J. Am. Chem. Soc.* **2008**, *130*, 1110. (j) Casey, C. P.; Bikzhanova, G. A.; Cui, Q.; Guzei, I. A. *J. Am. Chem. Soc.* **2005**, *127*, 14062-14071. (k) Samec, J. S. M.; Éll, A. H.; Åberg, J. B.; Privalov, T.; Eriksson, L. Bäckvall, J.-E. *J. Am. Chem. Soc.* **2006**, *128*, 14293-14305. (l) Casey, C. P.; Clark, T. B.; Guzei, I. A. *J. Am. Chem. Soc.* **2007**, *129*, 11821-11827. (m) Comas-Vives, A.; Ujaque, G.; Lledós, A. *Organometallics* **2008**, *27*, 4854-4863. (n) Casey, C. P.; Beetner, S. E.; Johnson, J. B. *J. Am. Chem. Soc.* **2008,** *130*, 2285-2295. (o) Conley, B. L.; Pennington-Boggio, M. K.; Boz, E.; Williams, T. J. *Chem. Rev.* **2010**, *110*, 2294-2312.

(4 ) For a recent study of ligand optimization for asymmetric induction see Imamoto, T.; Tamura, K.; Zhang, Z.; Horiuchi, Y.; Sugiya, M.; Yoshida, K.; Yanagisawa, A.; Gridnev, I. D. *J. Am. Chem. Soc.* **2012**, *134*, 1754-1769 and references therein.

(5) (a) Casey, C. P.; Guan, H. *J. Am. Chem. Soc.* **2007**, *129*, 5816-5817. (b) Casey, C. P.; Guan, H. *J. Am. Chem. Soc.* **2009**, *131*, 2499-2507. (c) Morris, R. H. *Chem. Soc. Rev.* **2009**, *38*, 2282-2291. (d) Zuo, W.; Lough, A. J.; Li, Y. F.; Morris, R. H. *Science* **2013,** *342*, 1080-1083.

(6) O, W. W. N.; Lough A. J.; Morris, R. H. *Organometallics* **2011**, *30*, 1236-1252.

(7) Comas-Vives, A.; Ujaque, G.; Lledós, A. *Adv. Inorg. Chem.* **2010**, *62*, 231-260.

(8) Alonso, D. A.; Brandt, P.; Nordin, S. J. M.; Andersson, P. G. *J. Am. Chem. Soc.* **1999**, *121*, 9580-9586.

(9) Yamakawa, M.; Ito, H.; Noyori, R. *J. Am. Chem. Soc.* **2000**, *122*, 1466 - 1478.

(10) Petra, D; G. I.; Reek, J. N. H.; Handgraaf, J.-W.; Meijer, E. J.; Dierkes, P.; Kramer, P. C. J.; Brussee, J.; Schoemacker, H. E.; van Leeuwen, P. W. N. M. *Chem. – Eur. J*. **2000**, *6,* 2818-2929.

(11) Abdur-Rashid, K.; Clapham, S. E.; Hadzovic, A.; Harvey, J. N.; Lough, A. J.; Morris, R. H. *J. Am. Chem. Soc.* **2002**, *124*, 15104-15118.

(12) Handgraaf, J.-W.; Reek, J. N. H.; Meijer, E. J. *Organometallics* **2003**, *22*, 3150-3157.

(13) Handgraaf, J.-W.; Meijer, E. J. *J. Am. Chem. Soc.* **2007**, *129*, 3099-3103.

(14) O, W. W. N.; Lough, A. J.; Morris, R. H. *Organometallics* **2012**, *31*, 2152-2165.

(15) Prokopchuk, D. E.; Morris, R. H. *Organometallics* **2012**, *31*, 7375-7385.

(16) Hasanayn, F.; Morris R. H. *Inorg. Chem.* **2012**, *51*, 10808-10818.

(17) Pavlova, A. Meijer, E.-J. *Chem. Phys. Chem.* **2012**, 13, 3492-3496.

(18) Zhang, X.; Guo, X.J.; Chen, Y.; Tang, Y. H.; Lei, M.; Fang, W. H. *Phys.Chem.Chem.Phys.* **2012**, *14*, 6003-6012.

(19) Dub, P. A.; Ikariya, T. *J. Am. Chem. Soc.* **2013**, *135*, 2604-2619.

(20) Schley, N. D.; Halbert, S.; Raynaud, C.; Eisenstein, O.; Crabtree, R. H. *Inorg. Chem.*, **2012**, *51*, 12313-12323.

(21) O, W. W. N.; Lough A. J.; Morris, R. H. *Organometallics* **2012**, *31*, 2137-2151.

(22) Fujii, A.; Hashiguchi, S.; Uematsu, N.; Ikariya, T.; Noyori, R. *J. Am. Chem. Soc.* **1996**, *118*, 2521-2522.

(23) Jiménez-Tenorio, M.; Puerta, M. C.; Valerga, P. *Eur. J. Inorg. Chem.* **2004**, 17-32.

(24) Murata, M.; Ikariya, T.; Noyori, R. *J. Org. Chem.* **1999**, *64*, 2186-2187.

(25) Haack, K.-J.; Hashiguchi, S.; Fujii, A.; Ikariya, T.; Noyori, R. *Angew. Chem. Int. Ed. Eng*. **1997**, *36*, 285-288.

(26) Mashima, K.; Abe, T.; Tani, K. *Chem. Lett.* **1998**, 1199-1200.

(27) (a) Blacker, A. J., Mellor, B., WO9842643A3, 1998. (b) Blacker, A. J.; Duckett, S. B.; Grace J.; Perutz, R. N.; Whitwood, A. C. *Organometallics* **2009**, *28*, 1435-1446.

(28) Mashima, K.; Abe, T.; Tani, K. *Chem. Lett.* **1998**, 1201-1202.

(29) Wu, X.; Liu, J.; Di Tommaso, D.; Iggo, J. A.; Catlow, C. R. A.; Bacsa, J.; Xiao, J. *Chem. –Eur. J.* **2008**, *14*, 7699-7715.

(30) Soni, R.; Cheung, F. K.; Clarkson, G. C.; Martins, J. E. D.; Graham M. A.: Wills, M. *Org. Biomol. Chem.* **2011**, *9*, 3290-3294.

(31) Espinet, P.; Bailey P. M.; Maitlis P. M. *J. Chem. Soc. Dalton Trans.* **1979**, 1542-1547.

(32) Blacker, A. J.; Clot, E.; Duckett, S. B.; Eisenstein, O.; Grace, J.; Nova, A.; Perutz, R. N.; Taylor, D. J.; Whitwood, A. C. *Chem. Commun.* **2009**, 6801-6803.

(33) Koike, T.; Ikariya, T. *Adv. Synth. Cat.* **2004**, *346*, 37-41.

(34) (a) Gaussian 03, Revision E.01, Frisch, M. J. *et al*. Gaussian, Inc., Wallingford CT, 2004. (b) Gaussian 09, Revision D.01, Frisch, M. J. *et al*. Gaussian, Inc., Wallingford CT, 2009.

(35) (a) Becke, A. D. *J. Chem. Phys.* **1993**, *98*, 5648–5662. (b) Perdew, J. P.; Wang, Y. *Phys. Rev. B* **1992**, *45*, 13244–13249.

(36) Andrae, D.; Häussermann, U.; Dolg, M.; Stoll, H.; Preuss, H. *Theor. Chim. Acta* **1990,** *77*, 123-141.

(37) Ehlers, A. W.; Böhme, M.; Dapprich, S.; Gobbi, A.; Höllwarth, A.; Jonas, V.; Köhler, K. F.; Stegmann, R.; Veldkamp, A.; Frenking, G. *Chem. Phys. Lett.* **1993**, *208,* 111-114.

(38) Hariharan, P. C.; Pople, J. A. *Theor. Chim. Acta* **1973,** *28*, 213-222.

(39) Bergner, A.; Dolg, M.; Küchle, W.; Stoll, H.; Preuss, H. *Mol. Phys.* **1993,** *80*, 1431-1441.

(40) Höllwarth, A.; Böhme, H.; Dapprich, S.; Ehlers, A. W.; Gobbi, A.; Jonas, V.; Köhler, K. F.; Stegmann, R.; Veldkamp, A.; Frenking, G. *Chem. Phys. Lett.* **1993,** *203*, 237-240.

(41) Reed, A. E.; Curtis, L. A.; Weinhold, F. *Chem. Rev.* **1988**, *88,* 899-926.

(42 ) Schmeier, T. J.; Dobereiner, G. E.; Crabtree, R. H.; Hazari, N. *J. Am. Chem. Soc.* **2011**, *133*, 9274-9277.

(43) (a) Martins, J. E. D.; Clarkson, G. J.; Wills, M. *Org. Lett.* **2009**, *11*, 847-850. (b) Cheung, F. K.; Clarke, A. J.; Clarkson, G. J.; Fox, D. J.; Graham, M. A.; Lin, C.; Crivillé, A. L.; Wills, M. *Dalton Trans.* **2010**, *39*, 1395-1402.

(44) Magee, M. P.; Norton, J. R. *J. Am. Chem. Soc.* **2001**, *123*, 1778-1779.
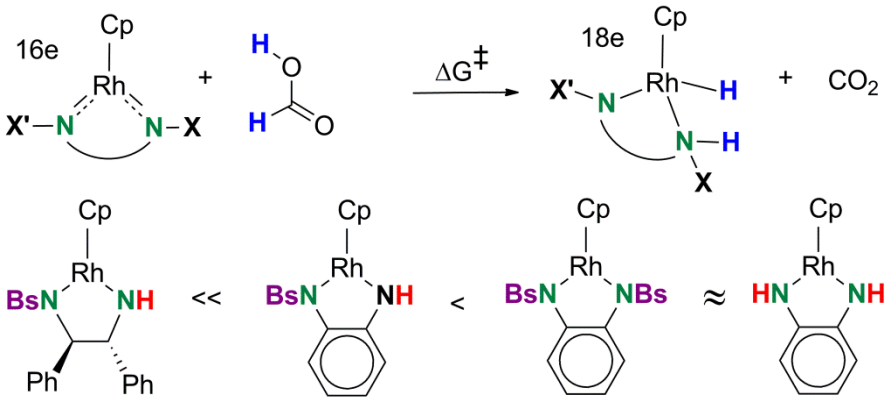
## Table of Contents Graphic